Phase field method for mean curvature flow with boundary constraints

Elie Bretin, Valérie Perrier

Phase field method for mean curvature flow with boundary constraints

Elie BRETIN
CMAP, Ecole Polytechnique, 91128 Palaiseau, France,
bretin@polytechnique.fr

Valerie PERRIER
LJK, CNRS, Université de Joseph Fourier, B.P. 53, 38041 Grenoble Cedex 9, France,
Valerie.Perrier@imag.fr

Abstract

This paper is concerned with the numerical approximation of mean curvature flow $t \to \Omega(t)$ satisfying an additional inclusion-exclusion constraint $\Omega_1 \subset \Omega(t) \subset \Omega_2$. Classical phase field model to approximate these evolving interfaces consists in solving the Allen-Cahn equation with Dirichlet boundary conditions. In this work, we introduce a new phase field model, which can be viewed as an Allen Cahn equation with a penalized double well potential. We first justify this method by a Γ-convergence result and then show some numerical comparisons of these two different models.

Introduction

In the last decades, a lot of work has been devoted to the motion of interfaces, and particularly to motion by mean curvature. Applications concern image processing (denoising, segmentation), material sciences (motion of grain boundaries in alloys, crystal growth), biology (modeling of vesicles and blood cells), image denoising, image segmentation and motion of grain boundaries.

Let us introduce the general setting of mean curvature flows. Let $\Omega(t) \subset \mathbb{R}^d$, $0 \leq t \leq T$, denote the evolution by mean curvature of a smooth bounded domain $\Omega_0 = \Omega(0)$: the outward normal velocity V_n at a point $x \in \partial\Omega(t)$ is given by

$$V_n = \kappa, \tag{1}$$

where κ denotes the mean curvature at x, with the convention that κ is negative if the set is convex. We will consider only smooth motions, which are well-defined if T is sufficiently small [3]. Since singularities may develop in finite time, one may need to consider the evolution in the sense of viscosity solutions [4, 13].

The evolution of $\Omega(t)$ is closely related to the minimization of the following energy:

$$J(\Omega) = \int_{\partial\Omega} 1 \, d\sigma.$$

Indeed, (1) can be viewed as a L^2-gradient flow of this energy.

Following [16, 15], the functional J can be approximated by a Ginzburg–Landau functional :

$$J_\epsilon(u) = \int_{\mathbb{R}^d} \left(\frac{\epsilon}{2} |\nabla u|^2 + \frac{1}{\epsilon} W(u) \right) dx.$$

where $\epsilon > 0$ is a small parameter, and W is a double well potential with wells located at 0 and 1 (for example $W(s) = \frac{1}{2} s^2 (1-s)^2$).

Modica and Mortola [16, 15] have shown the Γ-convergence of J_ϵ to $c_W J$ in $L^1(\mathbb{R}^d)$ (see also [5]), where

$$c_W = \int_0^1 \sqrt{2W(s)} ds. \tag{2}$$

The corresponding Allen–Cahn equation [2], obtained as the L^2-gradient flow of J_ϵ, reads

$$\frac{\partial u}{\partial t} = \Delta u - \frac{1}{\epsilon^2} W'(u). \tag{3}$$

Existence, uniqueness, and a comparison principle have been established for this equation (see for example chapters 14 and 15 in [3]). To this equation, one usually associates the profile

$$q = \arg\min \left\{ \int_{\mathbb{R}} \left(\frac{1}{2} \gamma'^2 + W(\gamma) \right) \; ; \; \gamma \in H^1_{loc}(\mathbb{R}), \; \gamma(-\infty) = 1, \; \gamma(+\infty) = 0, \; \gamma(0) = \frac{1}{2} \right\} \tag{4}$$

Remark 1. *The profile q (when W is continuous) can also be obtained [1] as the global decreasing solution of the following Cauchy problem*

$$\begin{cases} q'(s) = -\sqrt{W(s)}, & s \in \mathbb{R} \\ q(0) = \frac{1}{2}, \end{cases}$$

and satisfies

$$\int_{\mathbb{R}} \left(\frac{1}{2} q'(s)^2 + W(q(s)) \right) = \int_0^1 \sqrt{2W(s)} ds.$$

Then, the motion $\Omega(t)$ can be approximated by

$$\Omega_\epsilon(t) = \left\{ x \in \mathbb{R}^d \; ; \; u_\epsilon(x,t) \geq \frac{1}{2} \right\},$$

where u_ϵ is the solution of the Allen Cahn equation (3) with the initial condition

$$u_\epsilon(x,0) = q\Big(\frac{d(x, \Omega(0))}{\epsilon} \Big).$$

Here $d(x, \Omega)$ denotes the signed distance of a point x to the set Ω.

The convergence of $\partial\Omega_\epsilon(t)$ to $\partial\Omega(t)$ has been proved for smooth motions [12, 6] and in the general case without fattening [4, 13]. The convergence rate has been proved to behaves as $O(\epsilon^2 |\log \epsilon|^2)$.

From the practical point of view, this equation is usually solved in a box Q, with periodic boundary conditions, which allow solutions to be compute via a semi-implicit Fourier-spectral method as in the paper [11].

In this article, we investigate the approximation of interfaces evolving in a restricted area, which usually occurs in several physical applications. More precisely, we will consider mean curvature flow $t \to \Omega(t)$ evolving as the L^2 gradient flow of the following energy :

$$J_{\Omega_1,\Omega_2}(\Omega) = \begin{cases} \int_{\partial\Omega} 1 \, d\sigma & \text{if } \Omega_1 \subset \Omega \subset \Omega_2, \\ +\infty & \text{otherwise.} \end{cases}$$

Here Ω_1 and Ω_2 are two given smooth subsets of $\mathbb{R}^d$ such that $dist(\partial\Omega_1, \partial\Omega_2) > 0$. These evolving interfaces will clearly satisfy the following constraint $\Omega_1 \subset \Omega(t) \subset \Omega_2$.

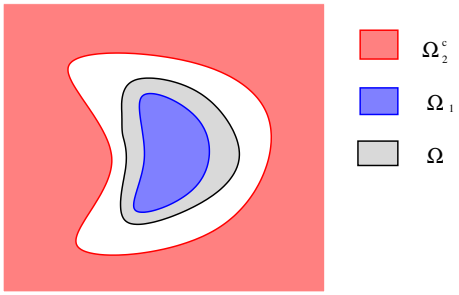

Figure 1: Constrained Mean curvature flow

Up to our knowledge, the only phase field model known to approximate these evolving interfaces considers the Allen Cahn equation in $\Omega_2 \setminus \Omega_1$ with Dirichlet boundary condition on $\partial\Omega_1$ and $\partial\Omega_2$ [17]. Yet, some limitations appear in this model :

- The Dirichlet boundary conditions prevent interfaces to reach boundaries $\partial\Omega_1$ and $\partial\Omega_2$. This can be seen as a consequence of thickness of the interface layer which is about $O(\epsilon \ln(\epsilon))$. This highlights the fact that the convergence rate of this model can not be better than $O(\epsilon \ln(\epsilon))$.

- From a numerical point of view, the resolution of the Allen Cahn equation with Dirichlet boundary conditions can be performed using a finite element method. This appears less efficient and more difficult to implement in dimensions greater than 2 than the semi-implicit Fourier-spectral method of [11].

To overcome these limitations, we introduce in this paper a new phase field model. The main idea will be to consider the Allen-Cahn equation in the whole domain with a penalization technique to take into account the boundary constraints.

The paper is organized as follows:

In section 2, we present in detail the two phase field model. In section 3, we justify our penalized approach by a Γ-convergence result. In section 4, we compare our method to the classical Finite Element model of [17], through numerical illustrations. These simulations will clarify the numerical convergence rate of each model.

1 Phase field model with boundary constraints

In this section, we will introduce our Allen Cahn model for the approximation of mean curvature flow $t \to \Omega(t)$ evolving as the L^2 gradient flow of the following energy

$$J_{\Omega_1,\Omega_2}(\Omega) = \begin{cases} \int_{\partial\Omega} 1 \, d\sigma & \text{if } \Omega_1 \subset \Omega \subset \Omega_2 \\ +\infty & \text{otherwise} \end{cases}$$

where Ω_1 and Ω_2 are two given smooth subsets of $\mathbb{R}^d$ satisfying $dist(\partial\Omega_1, \partial\Omega_2) > 0$. We begin with the description of the classical approach.

1.1 Classical model with Dirichlet boundary conditions

The classical strategy, see for instance [17, 7], consists in introducing the function space

$$X_{\Omega_1,\Omega_2} = \left\{ u \in H^1(\Omega_2 \setminus \Omega_1) \; ; \; u_{|\partial\Omega_1} = 1 \quad , u_{|\partial\Omega_2} = 0 \right\},$$

and a penalized Ginzburg-Landau energy of the form

$$\tilde{J}_{\epsilon,\Omega_1,\Omega_2}(u) = \begin{cases} \int_{\Omega_2\setminus\Omega_1} \left(\frac{\epsilon}{2} |\nabla u|^2 + \frac{1}{\epsilon} W(u) \right) dx & \text{if } u \in X_{\Omega_1,\Omega_2} \\ +\infty & \text{otherwise.} \end{cases}$$

In such framework, Chambolle and Bourdin [7] have shown the Γ-convergence of $\tilde{J}_{\epsilon,\Omega_1,\Omega_2}$ to $c_W J_{\Omega_1,\Omega_2}$ in $L^1(\mathbb{R}^d)$ (c_W has been introduced in (2)). This approximation conduces to the following Allen-Cahn equation

$$\begin{cases} u_t = \triangle u - \frac{1}{\epsilon^2} W'(u), & \text{on} \quad \Omega_2 \setminus \Omega_1 \\ u_{|\partial\Omega_1} = 1, \quad u_{|\partial\Omega_2} = 0 \\ u(0,x) = u_0 \in X_{\Omega_1,\Omega_2}. \end{cases}$$

A more general Γ-convergence result for the Allen-Cahn equation with Dirichlet boundary conditions can be found in [17].

1.2 Novel approach with a penalized double well potential

Now, we describe an alternative approach to force the boundary constraints, based on a penalized double well potential. From W considered in section 1.1, we define two continuous and positive potentials W_1 and W_2 satisfying the following assumption :

$$(H1) \begin{cases} W_1(s) = W(s) & \text{for } s \geq 1/2 \\ W_1(s) \geq \max(W(s), \lambda) & \text{for } s \leq 1/2 \end{cases} \quad \text{and} \quad \begin{cases} W_2(s) = W(s) & \text{for } s \leq 1/2 \\ W_2(s) \geq \max(W(s), \lambda) & \text{for } s \geq 1/2, \end{cases}.$$

where $\lambda > 0$.

For $\alpha > 1$, $\epsilon > 0$, and $x \in \mathbb{R}^d$, we introduce also a penalized double well potential $W_{\epsilon,\Omega_1,\Omega_2,\alpha}$ defined by

$$\begin{aligned} W_{\epsilon,\Omega_1,\Omega_2,\alpha}(s,x) \;\; = \;\; & W_1(s) \; q\left(\frac{dist(x,\Omega_1)}{\epsilon^\alpha} \right) + W_2(s) \; q\left(\frac{dist(x,\Omega_2^c)}{\epsilon^\alpha} \right) \\ & + W(s) \left(1 - q\left(\frac{dist(x,\Omega_1)}{\epsilon^\alpha} \right) - q\left(\frac{dist(x,\Omega_2^c)}{\epsilon^\alpha} \right) \right), \end{aligned} \tag{5}$$

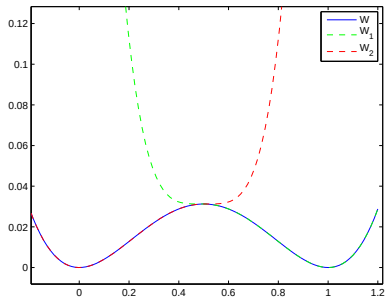

Figure 2: Example of potentials W, W_1 and W_2

where $dist(x, \Omega_1)$ and $dist(x, \Omega_2^c)$ are respectively the signed distance functions to the sets Ω_1 and Ω_2^c, and q is the profile function associated to W defined in (4).

Our modified Ginzburg-Landau energy $J_{\epsilon,\Omega_1,\Omega_2,\alpha}$ reads

$$J_{\epsilon,\Omega_1,\Omega_2,\alpha}(u) = \int_{\mathbb{R}^d} \left[\frac{\epsilon}{2} |\nabla u|^2 + \frac{1}{\epsilon} W_{\epsilon,\Omega_1,\Omega_2,\alpha}(u, x) \right] dx. \tag{6}$$

We will prove in the next section that this energy Γ-converges to $c_W J_{\Omega_1,\Omega_2}$. The associated Allen-Cahn equation reads in this context:

$$\begin{cases} \partial_t u(x,t) = \triangle u(x,t) - \frac{1}{\epsilon^2} \partial_s W_{\epsilon,\Omega_1,\Omega_2,\alpha}(u(x,t), x), & \text{for all } (x,t) \in \mathbb{R}^d \times [0, \infty(\\ u(0,x) = u_0(x) \end{cases}$$

2 Approximation result of the penalized Ginzburg-Landau energy

In this section, we prove the convergence of the Ginzburg-Landau energy $J_{\epsilon,\Omega_1,\Omega_2,\alpha}$ introduced in (6), to the following penalized perimeter

$$J_{\Omega_1,\Omega_2}(u) = \begin{cases} |Du|(\mathbb{R}^d) & \text{if } u = \mathbb{1}_\Omega \text{ and } \Omega_1 \subset \Omega \subset \Omega_2 \\ +\infty & \text{otherwise} \end{cases}.$$

Remark 2. *Given $u \in L^1(\mathbb{R}^d)$, $|Du|(\mathbb{R}^d)$ is defined by*

$$|Du|(\mathbb{R}^d) = \sup \left\{ \int_{\mathbb{R}^d} u \ \operatorname{div}(g) dx \ ; \ g \in C_c^1(\mathbb{R}^d, \mathbb{R}^d) \right\},$$

where $C_c^1(\mathbb{R}^d; \mathbb{R}^d)$ is the set of C^1 vector functions from $\mathbb{R}^d$ to $\mathbb{R}^d$ with compact support in $\mathbb{R}^d$. If $u \in W^{1,1}(\mathbb{R}^d)$, $|Du|$ coincides with the L^1-norm of ∇u and if $u = \mathbb{1}_\Omega$ where Ω has a smooth boundary, $|Du|$ coincides with the perimeter of Ω. Moreover, $u \to |Du|(\mathbb{R}^d)$ is lower semi-continuous in $L^1(\mathbb{R}^d)$ topology.

We assume in this section that Ω_1 and Ω_2 are two given smooth subsets of $\mathbb{R}^d$ satisfying $dist(\partial\Omega_1, \partial\Omega_2) > 0$, and that ϵ is sufficiently small such that

$$1 - q\left(\frac{dist(x, \Omega_1)}{\epsilon^\alpha}\right) - q\left(\frac{dist(x, \Omega_2^c)}{\epsilon^\alpha}\right) > 1/2, \tag{7}$$

for all x in $\Omega_2 \setminus \Omega_1$.

We now state the main result for the modified Ginzburg-Landau energy $J_{\epsilon,\Omega_1,\Omega_2,\alpha}$:

Theorem 1. *Assume that W is a positive double-well potential with wells located at 0 and 1, continuous on $\mathbb{R}$ and such that $W(s) = 0$ if and only if $s \in \{0,1\}$. Assume also that W_1 and W_2 are two continuous potentials satisfying assumption $(H1)$. Then, for any $\alpha > 1$, it holds*

$$\Gamma - \lim_{\epsilon \to 0} J_{\epsilon,\Omega_1,\Omega_2,\alpha} = c_W J_{\Omega_1,\Omega_2} \quad in \quad L^1(\mathbb{R}^d).$$

Proof. We first prove the liminf inequality.
i) *Liminf inequality :*
Let (u_ϵ) converge to u in $L^1(\mathbb{R}^d)$. As $J_{\epsilon,\Omega_1,\Omega_2,\alpha} \geq 0$, it is not restrictive to assume that the lim inf of $J_{\epsilon,\Omega_1,\Omega_2}(u_\epsilon)$ is finite. So we can extract a subsequence $u_n = u_{\epsilon_n}$ such that

$$\lim_{n \to +\infty} J_{\epsilon_h,\Omega_1,\Omega_2,\alpha}(u_n) = \liminf_{\epsilon \to 0} J_{\epsilon,\Omega_1,\Omega_2,\alpha}(u_\epsilon) \in \mathbb{R}^+.$$

Note that from remark (1) and assumption (7), it holds

$$\begin{cases} q\left(\frac{dist(x,\Omega_1)}{\epsilon^\alpha}\right) \geq 1/2 & \text{for } x \in \Omega_1, \\ q\left(\frac{dist(x,\Omega_2^c)}{\epsilon^\alpha}\right) \geq 1/2 & \text{for } x \in \Omega_2^c, \\ 1 - q\left(\frac{dist(x,\Omega_1)}{\epsilon^\alpha}\right) - q\left(\frac{dist(x,\Omega_2^c)}{\epsilon^\alpha}\right) \geq 1/2 & \text{for } x \in \Omega_2 \setminus \Omega_1, \\ 1 - q\left(\frac{dist(x,\Omega_1)}{\epsilon^\alpha}\right) - q\left(\frac{dist(x,\Omega_2^c)}{\epsilon^\alpha}\right) \geq 0 & \text{for } x \in \mathbb{R}^d, \end{cases}$$

for ϵ sufficiently small.

This implies that

$$\begin{aligned} \int_{\Omega_1} W_1(u_n)dx &\leq \int_{\Omega_1} 2q\left(\frac{dist(x,\Omega_1)}{\epsilon_n^\alpha}\right) W_1(u_n)dx \\ &\leq 2\int_{\mathbb{R}^d} W_{\epsilon_n,\Omega_1,\Omega_2,\alpha}(u_n,x)dx \\ &\leq 2\epsilon_h J_{\epsilon_n,\Omega_1,\Omega_2,\alpha}(u_n). \end{aligned}$$

In the same way :

$$\int_{\mathbb{R}^d \setminus \Omega_2} W_2(u_n)dx \leq 2\epsilon_n J_{\epsilon_n,\Omega_1,\Omega_2,\alpha}(u_n) \quad \text{and} \quad \int_{\Omega_2 \setminus \Omega_1} W(u_n)dx \leq 2\epsilon_n J_{\epsilon_n,\Omega_1,\Omega_2,\alpha}(u_n).$$

At the limit $n \to \infty$, the Fatou's Lemma and the continuity of W, W_1 and W_2 imply that $\int_{\Omega_1} W_1(u)dx = 0$, $\int_{\mathbb{R}^d \setminus \Omega_2} W_2(u)dx = 0$ and $\int_{\Omega_2 \setminus \Omega_1} W(u)dx = 0$. Recall also that W, W_1 and W_2, vanish respectively at $s = \{0,1\}$, $s = \{1\}$ and $s = \{0\}$. This means that

$$u(x) \in \begin{cases} \{1\} & \text{a.e in } \Omega_1 \\ \{0\} & \text{a.e in } \mathbb{R}^d \setminus \Omega_2 \\ \{0,1\} & \text{a.e in } \Omega_2 \setminus \Omega_1, \end{cases}$$

almost everywhere. Hence, we can represent u by $\mathbb{1}_\Omega$ for some Borel set $\Omega \in \mathbb{R}^d$ satisfying $\Omega_1 \subset \Omega \subset \Omega_2$. Using the Cauchy inequality, we can estimate

$$\begin{aligned} J_{\epsilon_n,\Omega_1,\Omega_2,\alpha}(u_n) &\geq \int_{\mathbb{R}^d} \left[\frac{\epsilon_n|\nabla u_h|^2}{2} + \frac{1}{\epsilon_n}W(u_n)\right] dx \quad (\text{ because } W_1 \geq W \text{ and } W_2 \geq W) \\ &\geq \int_{\mathbb{R}^d} \left[\frac{\epsilon_n|\nabla u_n|^2}{2} + \frac{1}{\epsilon_n}\tilde{W}(u_n)\right] dx \quad \left(\text{ where } \tilde{W}(s) = \min\left\{W(s)\ ;\ \sup_{s\in[0,1]} W(s)\right\}\right) \\ &\geq \int_{\mathbb{R}^d} \sqrt{2\tilde{W}(u_n)}|\nabla u_n|dx = \int_{\mathbb{R}^d} |\nabla[\phi(u_n)]|dx = |D[\phi(u_n)]|(\mathbb{R}^d), \end{aligned}$$

where $\phi(s) = \int_0^s \sqrt{2\tilde{W}(t)}dt$. Since ϕ is a Lipschitz function (because $\tilde{W}$ is bounded), $\phi(u_\epsilon)$ converges in $L^1(\mathbb{R}^d)$ to $\phi(u)$. Using the lower semicontinuity of $v \to |Dv|(\mathbb{R}^d)$, we obtain

$$\lim_{n\to+\infty} J_{\epsilon_n,\Omega_1,\Omega_2}(u_n) \geq \liminf_{n\to+\infty} |D\phi(u_n)|(\mathbb{R}^d) \geq |D\phi(u)|(\mathbb{R}^d).$$

The lim inf inequality is finally obtained remarking that $\phi(u) = \phi(\mathbb{1}_\Omega) = c_W \mathbb{1}_\Omega = c_W u$.

Let us now prove the limsup inequality.
ii) *Limsup inequality :*
We first assume that $u = \mathbb{1}_\Omega$ for some bounded open set Ω satisfying $\Omega_1 \subset \Omega \subset \Omega_2$ with smooth boundaries. We introduce the sequence

$$u_\epsilon(x) = q\left(\frac{dist(x,\Omega)}{\epsilon}\right).$$

and two constants c_1 and c_2 defined by

$$c_1 = \sup_{s\in[0,1]} \{W_1(s) - W(s)\}, \quad \text{and} \quad c_2 = \sup_{s\in[0,1]} \{W_1(s) - W(s)\}.$$

Note that

$$\begin{aligned} J_{\epsilon,\Omega_1,\Omega_2,\alpha}(u_\epsilon) &= \int_{\mathbb{R}^d} \left[\frac{\epsilon|\nabla u_\epsilon|^2}{2} + \frac{1}{\epsilon}W(u_\epsilon)\right] dx + \int_{\mathbb{R}^d} \frac{1}{\epsilon} q\left(\frac{dist(x,\Omega_1)}{\epsilon^\alpha}\right)(W_1(u_\epsilon) - W(u_\epsilon))\, dx \\ &\quad + \int_{\mathbb{R}^d} \frac{1}{\epsilon} q\left(\frac{dist(x,\Omega_2^c)}{\epsilon^\alpha}\right)(W_2(u_\epsilon) - W(u_\epsilon))\, dx \end{aligned}$$

Each of these 3 terms above is now analyzed.

1) Estimation of the first term :

$$\mathcal{I}_\epsilon^1 = \int_{\mathbb{R}^d} \left[\frac{\epsilon|\nabla u_\epsilon|^2}{2} + \frac{1}{\epsilon}W(u_\epsilon)\right] dx.$$

By co-area formula, we estimate

$$\begin{aligned} \mathcal{I}_\epsilon^1 &= \frac{1}{\epsilon}\int_{\mathbb{R}^d} \left[\frac{q'(d(x,\Omega)/\epsilon)^2}{2} + W(q(d(x,\Omega)/\epsilon))\right] dx \\ &= \frac{1}{\epsilon}\int_{\mathbb{R}} g(s) \left[\frac{q'(s/\epsilon)^2}{2} + W(q(s/\epsilon))\right] ds \\ &= \int_{\mathbb{R}} g(\epsilon t) \left[\frac{q'(t)^2}{2} + W(q(t))\right] dt \end{aligned}$$

where $g(s) = |D\mathbb{1}_{\{d\leq s\}}|(\mathbb{R}^d)$.
By the smoothness of $\partial\Omega$, $g(\epsilon t)$ converges to $|D\mathbb{1}_{\{dist(x,\Omega)\leq 0\}}|(R^d)$ as $\epsilon \to 0$; moreover, by definition of the profile q, u_ϵ converges to $\mathbb{1}_\Omega$ and

$$\limsup_{\epsilon\to 0} \mathcal{I}_\epsilon^1 \leq |D\mathbb{1}_\Omega|(\mathbb{R}^d) \int_{-\infty}^{+\infty} \left[\frac{1}{2}|q'(s)|^2 + W(q(s))ds\right].$$

According to remark (1), it follows that

$$\int_{-\infty}^{+\infty} \left[\frac{1}{2}|q'(s)|^2 + W(q(s))\right] ds = \int_0^1 \sqrt{2W(s)}ds = c_W,$$

which implies that

$$\limsup_{\epsilon\to 0} \mathcal{I}_\epsilon^1 \leq c_W |D\mathbb{1}_\Omega|(\mathbb{R}^d).$$

2) Estimation of the second term :

$$\mathcal{I}_\epsilon^2 = \int_{\mathbb{R}^d} \frac{1}{\epsilon} q\left(\frac{dist(x,\Omega_1)}{\epsilon^\alpha}\right)(W_1(u_\epsilon) - W(u_\epsilon))\,dx.$$

The function $dist(x,\Omega)$ is negative on Ω_1, thus $u_\epsilon(x) \geq \frac{1}{2}$ on Ω_1 and $W_1(u_\epsilon(x)) = W(u_\epsilon(x))$ for all $x \in \Omega_1$. This means that

$$\mathcal{I}_\epsilon^2 = \int_{\mathbb{R}^d\setminus\Omega_1} \frac{1}{\epsilon} q\left(\frac{dist(x,\Omega_1)}{\epsilon^\alpha}\right)(W_1(u_\epsilon) - W(u_\epsilon))\,dx \leq c_1 \int_{\mathbb{R}^d\setminus\Omega_1} \frac{1}{\epsilon} q\left(\frac{dist(x,\Omega_1)}{\epsilon^\alpha}\right)dx,$$

where $c_1 = \sup_{s\in[0,1]}\{W_1(s) - W(s)\}$.
Using co-area formula, we estimate

$$\int_{\mathbb{R}^d\setminus\Omega_1} \frac{1}{\epsilon} q\left(\frac{dist(x,\Omega_1)}{\epsilon^\alpha}\right)dx = \int_0^\infty \frac{1}{\epsilon} g_1(s) q\left(\frac{s}{\epsilon^\alpha}\right)ds = \epsilon^{\alpha-1}\int_0^\infty g_1(\epsilon^\alpha s) q(s) ds,$$

where $g_1(s) = |D\mathbb{1}_{\{dist(x,\Omega_1)\leq s\}}|(\mathbb{R}^d)$.
By the smoothness of Ω_1, $g(\epsilon^\alpha t)$ converges to $|D\mathbb{1}_{dist(x,\Omega_1)\leq 0}|(R^d)$ as $\epsilon \to 0$. We then deduce that

$$\limsup_{\epsilon\to 0} \mathcal{I}_\epsilon^2 = 0,$$

as $\alpha > 1$ and $\int_0^\infty q(s)ds$ is bounded.

3) Estimation of the last term :

$$\mathcal{I}_\epsilon^3 = \int_{\mathbb{R}^d} \frac{1}{\epsilon} q\left(\frac{dist(x,\Omega_2^c)}{\epsilon^\alpha}\right)(W_2(u_\epsilon) - W(u_\epsilon))\,dx.$$

This estimation is similar to the second one. The function $dist(x,\Omega)$ is positive on $\mathbb{R}^d \setminus \Omega_2$, this means $u_\epsilon(x) \leq \frac{1}{2}$ on $\mathbb{R}^d \setminus \Omega_2$ and $W_2(u_\epsilon(x)) = W(u_\epsilon(x))$ for all $x \in \mathbb{R}^d \setminus \Omega_2$. Then, we have

$$\mathcal{I}_\epsilon^3 = \int_{\Omega_2} \frac{1}{\epsilon} q\left(\frac{dist(x,\Omega_2^c)}{\epsilon^\alpha}\right)(W_2(u_\epsilon) - W(u_\epsilon))\,dx \leq c_2 \int_{\Omega_2} \frac{1}{\epsilon} q\left(\frac{dist(x,\Omega_2^c)}{\epsilon^\alpha}\right)dx,$$

and using co-area formula, it holds

$$\int_{\Omega_2} \frac{1}{\epsilon} q\left(\frac{dist(x,\Omega_2^c)}{\epsilon^\alpha}\right)dx = \int_0^\infty \frac{1}{\epsilon} g_2(s) q\left(\frac{s}{\epsilon^\alpha}\right)ds = \epsilon^{\alpha-1}\int_0^\infty g_2(\epsilon^\alpha s) q(s) ds,$$

where $g_2(s) = |D\mathbb{1}_{\{dist(x,\Omega_2)\leq -s\}}|(\mathbb{R}^d)$. We deduce as before that

$$\limsup_{\epsilon\to 0} \mathcal{I}_\epsilon^3 = 0.$$

Finally, we conclude that

$$\limsup_{\epsilon\to 0} J_{\epsilon,\Omega_1,\Omega_2,\alpha}(u_\epsilon) \leq c_W |D\mathbb{1}_\Omega|(\mathbb{R}^d).$$

□

Remark 3. *This theorem is still true in the limit case $\alpha \to \infty$, where $J_{\epsilon,\Omega_1,\Omega_2,\alpha=\infty}(u)$ reads*

$$\begin{aligned} J_{\epsilon,\Omega_1,\Omega_2,\infty}(u) &= \int_{\Omega_1} \left[\frac{\epsilon|\nabla u|^2}{2} + \frac{1}{\epsilon} W_1(u) \right] dx + \int_{\Omega_2 \setminus \Omega_1} \left[\frac{\epsilon|\nabla u|^2}{2} + \frac{1}{\epsilon} W(u) \right] dx \\ &+ \int_{\mathbb{R}^d \setminus \Omega_2} \left[\frac{\epsilon|\nabla u|^2}{2} + \frac{1}{\epsilon} W_2(u) \right]. \end{aligned}$$

3 Algorithms and numerical simulations

We now compare numerically the two phase field models described previously. The first and classical model is integrated by a semi-implicit finite element method whereas our penalized Allen Cahn equation is solved by the semi-implicit Fourier spectral algorithm. In particular, we will observe that both approaches give similar solutions but,

- the algorithm used for the penalized Allen Cahn equation is more efficient and has lower complexity than the semi-implicit finite element method used for the Allen Cahn equation with Dirichlet boundary conditions.

- the convergence rate of the phase field approximation appears to behave as about $O(\epsilon \ln(\epsilon))$ for the first model and as $O(\epsilon^2 \ln(\epsilon)^2)$ for our penalized version of Allen Cahn equation.

3.1 A semi-implicit finite element method for the Allen Cahn equation with Dirichlet boundary conditions

Let us give more precision about the classic semi-implicit finite element method used for the equation

$$u_t(x,t) = \Delta u(x,t) - \frac{1}{\epsilon^2} W'(u)(x,t), \quad \text{on} \quad \Omega_2 \setminus \Omega_1 \times [0,T], \tag{8}$$

where $u_{|\partial\Omega_1} = 1$, $u_{|\partial\Omega_2} = 0$ and $W(s) = \frac{1}{2} s^2 (1-s)^2$.

Note that when the initial condition u_0 is chosen of the form $u_0 = q\left(dist(\Omega_0, x)/\epsilon\right)$ with Ω_0 satisfying the constraint $\Omega_1 \subset \Omega_0 \subset \Omega_2$, then we expect that the set $\Omega^\epsilon(t)$ defined by

$$\Omega^\epsilon(t) = \Omega_1 \cup \{x \in \Omega_2 \setminus \Omega_1 \ ; \ u(x,t) \geq 1/2\},$$

should be a good approximation to the constraint mean curvature flow $t \to \Omega(t)$.

Let us introduce a triangulation mesh $\mathcal{T}_h$ on the set $\Omega_2 \setminus \Omega_1$ and the discretization time step δ_t. Then, we consider the approximation spaces $X_{h,0}$ and X_h defined by

$$\begin{cases} X_h &= \left\{ v \in H^1(\overline{\Omega_2 \setminus \Omega_1}) \cup C^0(\overline{\Omega_2 \setminus \Omega_1}) \ ; \ v_{|K \in \mathcal{T}_h} \in P_k(K), \quad v_{|\Omega_1} = 1 \text{ and } v_{|\Omega_2} = 0 \right\} \\ X_{h,0} &= \left\{ v \in H_0^1(\Omega_2 \setminus \Omega_1) \cup C^1(\Omega_2 \setminus \Omega_1) \ ; \ v_{|K \in \mathcal{T}_h} \in P_2(K) \right\} \end{cases}$$

where P_k denotes the polynomial space of degree k. We take $k = 2$ in the future numerical illustrations. Then, the solution $u(x, t_n)$ at time $t_n = n\delta_t$ is approximated by $U^{h,n}$, defined for $n > 1$ as the solution on X_h of

$$\int_{\Omega_2\setminus\Omega_1} U^{h,n}\varphi\, dx + \delta_t \int_{\Omega_2\setminus\Omega_1} \nabla U^{h,n}\nabla\varphi\, dx = \int_{\Omega_2\setminus\Omega_1} \left(U^{h,n-1} - \frac{\delta_t}{\epsilon^2} W'(U^{h,n-1})\right)\varphi\, dx, \quad \forall\varphi \in X_{h,0},$$

and for $n = 0$ by

$$U^{h,0} = \arg\min_{v\in X_h} \|v - u_0\|_{L^2(\Omega_2\setminus\Omega_1)}.$$

This algorithm is known to be stable under the condition

$$\delta_t \;\leq\; c_W \epsilon^2,$$

where $c_W = \left[\sup_{t\in[0,1]} \{W''(s)\}\right]^{-1}$. More results about stability and convergence of this algorithm can be found in [14, 8].

3.2 A time-splitting Fourier spectral method for the penalized Allen-Cahn equation

We now consider the second model

$$u_t(x,t) = \triangle u(x,t) - \frac{1}{\epsilon^2}\partial_s W_{\epsilon,\Omega_1,\Omega_2,\alpha}(u)(x,t), \quad \text{on} \quad Q\times[0,T], \tag{9}$$

with periodic boundary conditions on a given box Q, chosen sufficiently large to contain Ω_2. In future numerical tests, we use $\alpha = 2$, $W(s) = \frac{1}{2}s^2(1-s)^2$ and the potentials W_1, W_2 are defined by

$$W_1(s) = \begin{cases} \frac{1}{2}s^2(1-s)^2 & \text{if } s \geq \frac{1}{2} \\ 10(s-0.5)^4 + 1/32 & \text{otherwise} \end{cases} \quad \text{and} \quad W_2(s) = \begin{cases} \frac{1}{2}s^2(1-s)^2 & \text{if } s \leq \frac{1}{2} \\ 10(s-0.5)^4 + 1/32 & \text{otherwise} \end{cases},$$

which clearly satisfy the assumption $(H1)$ (see figure (2)).

The initial condition u_0 satisfies $u_0 = q\left(dist(\Omega_0, x)/\epsilon\right)$ and we will show that the set

$$\Omega^\epsilon(t) = \{x \in Q \;;\; u(x,t) \geq 1/2\},$$

will be a good approximation of $\Omega(t)$ as ϵ tends to zero.

Our numerical scheme for solving equation (9) is based on a splitting method between the diffusion and reaction terms. We take advantage of the periodicity of u by integrating exactly the diffusion term in the Fourier space. More precisely, the solution $u(x, t_n)$ at time $t_n = t_0 + n\delta_t$ is approximated by its truncated Fourier series :

$$u_P^n(x) \;=\; \sum_{|p|_\infty = P} c_p^n e^{2i\pi p\cdot x}.$$

Here $|p|_\infty = \max_{1\leq i\leq d} |p_i|$ and P represents the number of Fourier modes in each direction.

The step n of our algorithm writes :

- $u_P^{n+1/2}(x) = \sum c_p^{n+1/2}\; e^{2i\pi p\cdot x}, \quad \text{with} \quad c_p^{n+1/2} = c_p^n\; e^{-4\pi^2\delta t\,|p|^2}.$

- $u_P^{n+1} = u_P^{n+1/2} - \frac{\delta t}{\epsilon^2}\partial_s W_{\epsilon,\Omega_2,\Omega_1\alpha}(u_P^{n+1/2})$.

In practice, the first step is performed via a Fast Fourier Transform, with a computational cost $O(P^d \ln(P))$. In the simplest case of traditional Allen Cahn equation, the corresponding numerical scheme turns out to be stable under the condition

$$\delta t \quad \leq \quad c_W \epsilon^2,$$

and the convergence of this splitting approach has been established in [10].

3.3 Simulations and numerical convergence

We compare in this part numerical solutions obtained with these two algorithms. For each test, we took $\epsilon = 2^{-8}$ and $\delta_t = \epsilon^2$. The P_2 finite element algorithm was implemented in Freefem++. The mesh $\mathcal{T}_h$ used in these simulations are plotted in figure (3). The penalization method was implemented in MATLAB where we have taken $P = 2^8$.

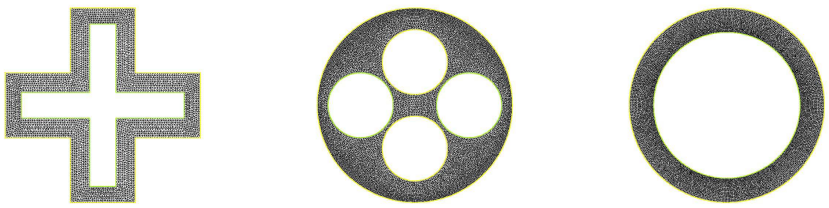

Figure 3: Mesh $\mathcal{T}_h$ generated by Freefem++, and used in simulations plotted on figures (4) and (5). In both cases, $\partial\Omega_1$ and $\partial\Omega_2$ are respectively identified as the green and the yellow boundaries.

We first plot two situations on figures (4) and (5). The functions u_ϵ are plotted only on the admissible set $\Omega_2 \setminus \Omega_1$ for the FE Dirichlet method and on all the set Q for the pseudo-spectral penalization version. We note that the solutions obtained by both methods are very similar.

In order to estimate the convergence rate of both models, we consider the case where Ω_1 and Ω_2 are two circles of radii equal to $R_1 = 0.3$ and $R_2 = 0.4$. The situation is thus very simple when the initial set Ω_0 is also a circle with radius R_0 satisfying $R_1 < R_0 < R_2$. Indeed, the penalized mean curvature motion $\Omega(t)$ evolves as a circle, with radius satisfying

$$R(t) = \max\left(\sqrt{R_0^2 - 2t}, R_1\right),$$

that decreases until $R(t) = R_1$.

The solutions of the two different models are computed for different values of ϵ with $P = 2^8$, $\delta_t = 1/P^2$ and $R_0 = 0.35$. In both cases, the set $\Omega^\epsilon(t)$ appears as a circle of radius $R^\epsilon(t)$. We then estimate the numerical error between $R^\epsilon(t)$ and $R(t)$. The results obtained for the first method are plotted on figure (6): the first figure corresponds to the evolution $t \to \mathbb{R}^\epsilon(t)$ for 4 different values of ϵ and the second figure shows the error

$$\epsilon \to \sup_{t\in[0,T]} \{|R(t) - R^\epsilon(t)|\},$$

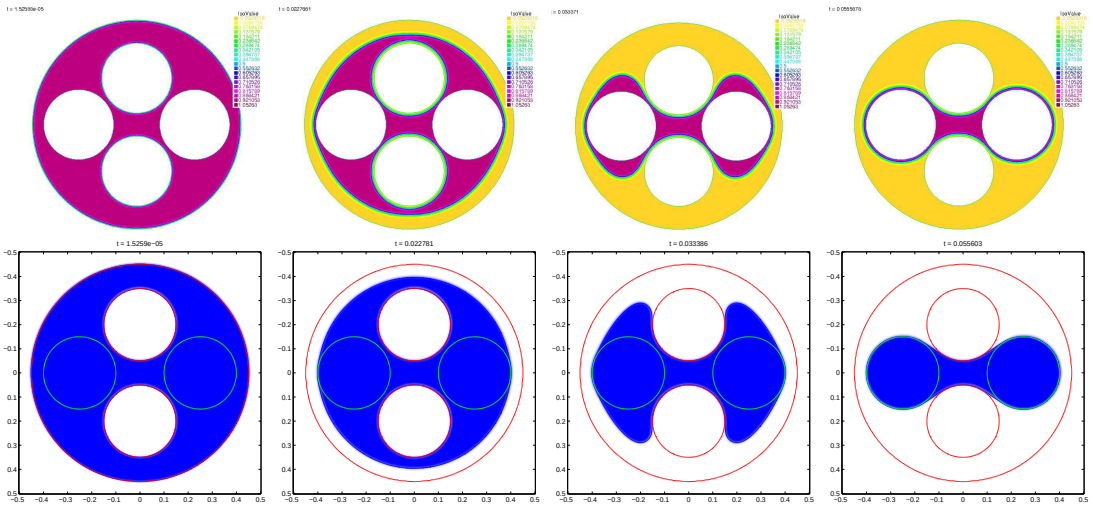

Figure 4: Numerical solutions obtained at different times $t_0 = 0$, $t_1 = 0.022$, $t_2 = 0.033$ and $t = 0.055$. The first line corresponds to the FE Dirichlet method and the second line to the penalization pseudo-spectral approach.

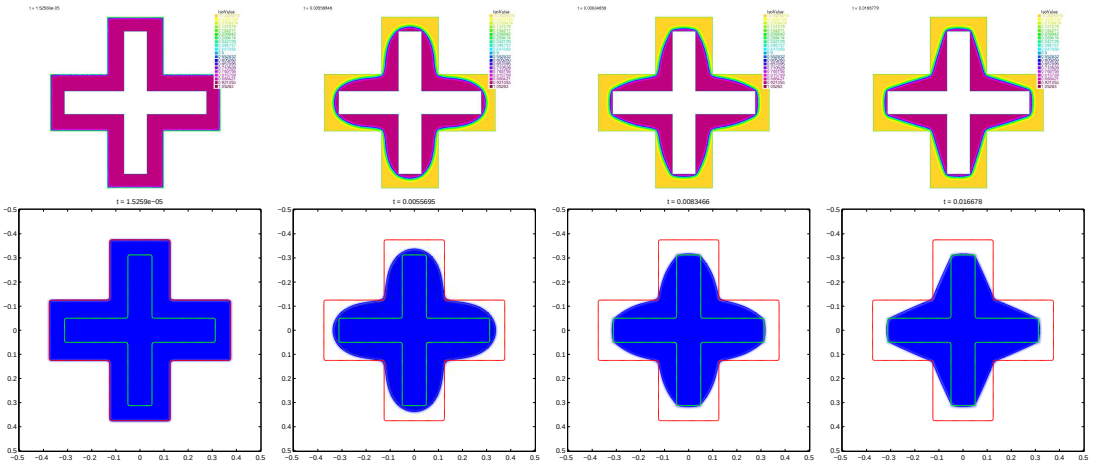

Figure 5: Numerical solutions obtained at different times $t_0 = 0$, $t_1 = 0.0055$, $t_2 = 0.0083$ and $t_3 = 0.016$. The first line corresponds to the FE Dirichlet method and the second line to the penalization pseudo-spectral approach.

in logarithmic scale. It clearly appears an error of $O(\epsilon \ln(\epsilon))$.
The same test is done for the penalization algorithm: the results are plotted on figure (7) and we now clearly observed a convergence rate of $O(\epsilon^2 \ln(\epsilon^2))$.

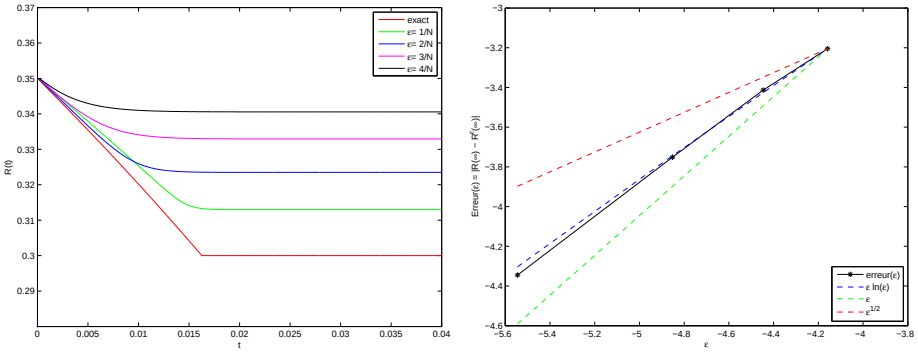

Figure 6: Dirichlet algorithm : numerical error $|R^\epsilon(t) - R(t)|$; Left: $t \to R^\epsilon(t)$ for different values of ϵ; Right: $\epsilon \to \sup_{t\in[0,T]} \{|R(t) - R^\epsilon(t)|\}$ in logarithmic scale.

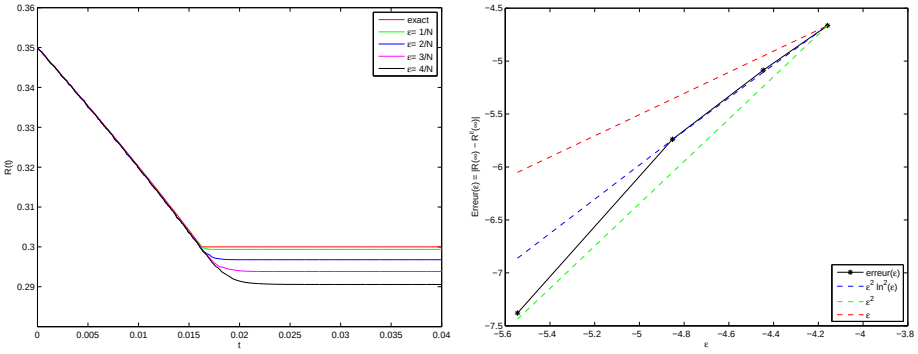

Figure 7: Penalization algorithm : numerical error $|R^\epsilon(t) - R(t)|$; Left: $t \to R^\epsilon(t)$ for different values of ϵ; Right: $\epsilon \to \sup_{t\in[0,T]} \{|R(t) - R^\epsilon(t)|\}$ in logarithmic scale.

Moreover, our approach allows us to simulate very easily and efficiently three dimensional experiments, whatever the geometry of the sets Ω_1 and Ω_2. See for instance figure (8) where the numerical solution of the Allen Cahn equation is plotted for different times t.

3.4 Possible extension of the method

Another advantage of our penalization approach is that it can be easily extended for more general situations of evolving interfaces. For example, we have recently considered a mean curvature flow with an additional forcing term g and a conservation of the volume in [9]. Then, the model of [9] can be modified to take into account additional inclusion-exclusion constraints by simply using potential W_{Ω_1,Ω_2} instead of W in phase field equation. In this case, this leads to the following perturbed Allen-Cahn equation

$$u_t = \Delta u - \frac{1}{\epsilon^2} F(u),$$

with

$$F(u) = W'_{\Omega_1,\Omega_2}(u) - \epsilon g \sqrt{2W_{\Omega_1,\Omega_2}(u)} - \frac{\int_Q W'_{\Omega_1,\Omega_2}(u) - \epsilon g \sqrt{2W_{\Omega_1,\Omega_2}(u)} dx}{\int_Q \sqrt{2W_{\Omega_1,\Omega_2}(u)} dx} \sqrt{2W_{\Omega_1,\Omega_2}(u)}.$$

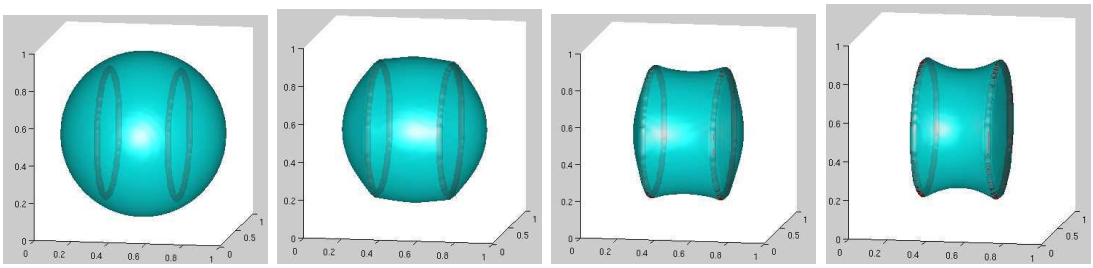

Figure 8: Minimal surface estimation : solution of the Allen Cahn equation at different times t. The domain Ω_1 is the union of the two red tores and Ω_2 is the box Q with $N = 2^7$, $\epsilon = 1/N$ and $\delta_t = \epsilon^2$

Two simulations obtained from this model are plotted in figure (9). We can observe that both constraints (conservation of the volume and inclusion-exclusion set) are well respected.

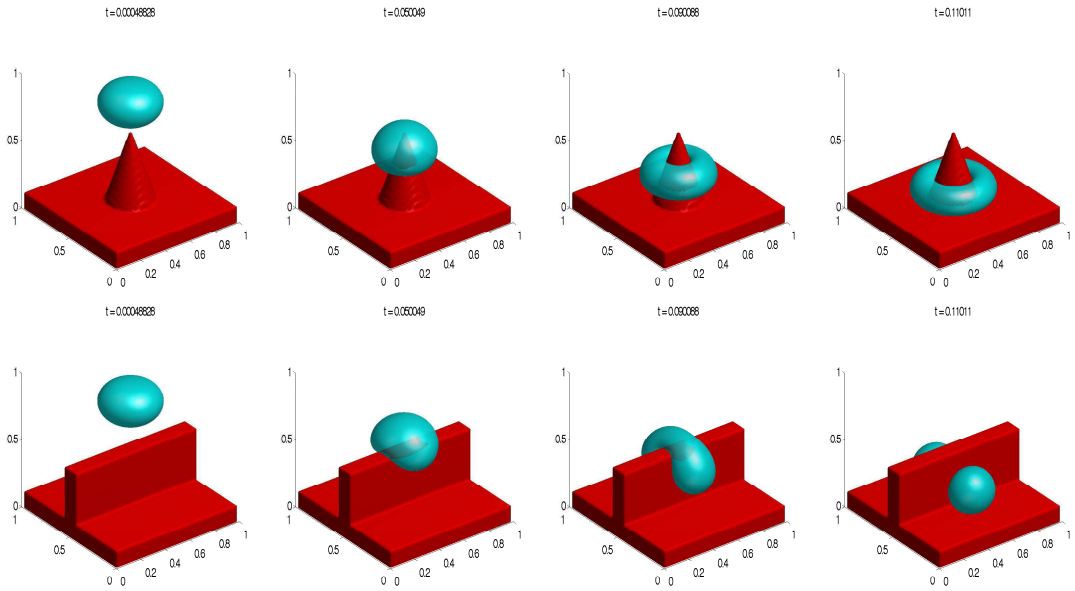

Figure 9: Two numerical experiments with a forcing term (gravity force), a volume conservation and an exclusion constraint : the domain Ω_1 is empty and Ω_2 is plotted in red in each picture. We used $N = 2^7$, $\epsilon = 1/N$ and $\delta_t = \epsilon^2$.

4 Conclusion

This paper has presented a new phase field model for the approximation of mean curvature flow with inclusion-exclusion constraints. The classical method in such situation consists to solve the Allen-Cahn equation with Dirichlet boundary conditions. Since this method appears to be not optimal while its convergence is observed with a rate about $O(\epsilon \ln(\epsilon))$ only, we have introduced a new approach based on a penalized double well potential. This method was firstly motivated by a Γ-convergence result and secondly numerical tests suggesting that its convergence rate is about $O(\epsilon^2 \ln(\epsilon)^2)$. The proof of the numerical precision of the scheme is still an open problem and will be the subject of a forthcoming paper. Another advantage of our method lies in its simplicity to be implemented, since it is only based on Fourier Transforms. This simplicity

allows to consider 3D Geometries, and to elaborate new strategies in more general situations, such as mean curvature flow with forcing term and conservation of volume.

References

[1] G. Alberti. Variational models for phase transitions, an approach via γ-convergence. In *Calculus of variations and partial differential equations (Pisa, 1996)*, pages 95–114. Springer, Berlin, 2000.

[2] S. M. Allen and J. W. Cahn. A microscopic theory for antiphase boundary motion and its application to antiphase domain coarsening. *Acta Metall.*, 27:1085–1095, 1979.

[3] L. Ambrosio. Geometric evolution problems, distance function and viscosity solutions. In *Calculus of variations and partial differential equations (Pisa, 1996)*, pages 5–93. Springer, Berlin, 2000.

[4] G. Barles. *Solutions de viscosité des équations de Hamilton-Jacobi*, volume 17 of *Mathématiques & Applications (Berlin) [Mathematics & Applications]*. Springer-Verlag, Paris, 1994.

[5] G. Bellettini. Variational approximation of functionals with curvatures and related properties. *J. Convex Anal.*, 4(1):91–108, 1997.

[6] G. Bellettini and M. Paolini. Quasi-optimal error estimates for the mean curvature flow with a forcing term. *Differential Integral Equations*, 8(4):735–752, 1995.

[7] B. Bourdin and A. Chambolle. Design-dependent loads in topology optimization. *ESAIM: Control, Optimisation and Calculus of Variations*, 9:19–48, 2003.

[8] M. Brassel. *Instabilité de Forme en Croissance Cristalline*. PhD thesis, University Joseph Fourier, Grenoble, 2008.

[9] M. Brassel and E. Bretin. A modified phase field approximation for mean curvature flow with conservation of the volume. Rapport de recherche arXiv:0904.0098v1, LJK, 2009. submitted.

[10] E. Bretin. *Méthode de champ de phase et mouvement par courbure moyenne*. PhD thesis, Institut national polytechnique de Grenoble, 2009.

[11] L. Chen and J. Shen. Applications of semi-implicit Fourier-spectral method to phase field equations. *Computer Physics Communications*, 108:147–158, 1998.

[12] X. Chen. Generation and propagation of interfaces for reaction-diffusion equations. *J. Differential Equations*, 96(1):116–141, 1992.

[13] L. C. Evans, H. M. Soner, and P. E. Souganidis. Phase transitions and generalized motion by mean curvature. *Comm. Pure Appl. Math.*, 45(9):1097–1123, 1992.

[14] X. Feng and A. Prohl. Numerical analysis of the Allen-Cahn equation and approximation for mean curvature flows. *Numerische Mathematik*, 94:33–65, 2003.

[15] L. Modica and S. Mortola. Il limite nella Γ-convergenza di una famiglia di funzionali ellittici. *Boll. Un. Mat. Ital. A (5)*, 14(3):526–529, 1977.

[16] L. Modica and S. Mortola. Un esempio di Γ^--convergenza. *Boll. Un. Mat. Ital. B (5)*, 14(1):285–299, 1977.

[17] N. C. Owen, J. Rubinstein, and P. Sternberg. Minimizers and gradient flows for singularly perturbed bi-stable potentials with a dirichlet condition. *Proceedings of the Royal Society of London. Series A, Mathematical and Physical Sciences*, 429(1877):pp. 505–532, 1990.